NOTES AND CORRESPONDENCE

The Meandering Path of a Drifter around the Western Alboran Gyre

JESÚS GARCÍA LAFUENTE AND JAVIER DELGADO

Department of Applied Physics II, University of Málaga, Málaga, Spain

7 March 2003 and 5 August 2003

ABSTRACT

An accidentally released drifter in the eastern section of the Strait of Gibraltar, whose successive positions were tracked by the Argos surveillance system, was advected more than 170 km around the western Alboran gyre in the Alboran Sea of the western Mediterranean Sea during four days. The drifter trajectory along the gyre's periphery was wavelike around a hypothetical smoothed streamline, with a period of 35 h and an amplitude of approximately 2 km. Temperature observations confirm the wavelike nature of the trajectory. Neither tidal currents within the Alboran basin nor wind-related forcing are able to explain the observed path. The interaction of the incoming Atlantic jet and the western Alboran gyre at the place where they meet together with the existence of relative vorticity pulses of the Atlantic jet associated with tidal currents in the strait is put forward as a likely mechanism that generates short-scale eddies in which the drifter could have been trapped. The subsequent advection of such an eddy around the gyre would depict the observed wavelike trajectory.

1. Introduction

The jet of Atlantic water (AJ) that comes into the Mediterranean Sea through the Strait of Gibraltar usually encounters a large anticyclonic gyre [western Alboran gyre (WAG)] that occupies the western subbasin of the Alboran Sea (Fig. 1). These structures are coupled to each other to form a typical pattern of surface circulation with a more or less developed WAG (identified by closed geostrophic streamlines in data analysis of hydrographic surveys), the AJ flowing around the WAG and eastward. The AJ may describe another meander around a second anticyclonic gyre in the eastern Alboran Sea [see Parrilla and Kinder (1987) for a general description of this area or Viúdez et al. (1998) for interesting insights of the general circulation with updated references].

The mentioned description is far from steady. The actual scenario is highly variable (Heburn and La Violette 1990; García Lafuente et al. 1998), ranging from the absence of both gyres with the AJ flowing as a coastal jet attached to the African coast to the presence of three simulataneous anticyclonic gyres (Viúdez et al. 1998; Vargas Yáñez et al. 2002). The properties of the AJ as it leaves the Strait of Gibraltar are even more variable. Sarhan et al. (2000) showed noticeable variations of few days period in the angle under which the AJ enters the Alboran basin. Meteorological forcing over the Mediterranean Sea induces inflow variations that may change the speed of the AJ by a factor greater than 3 at subinertial frequencies (Candela et al. 1989; García Lafuente et al. 2002). Tidal forcing changes the current velocity of the AJ at higher frequencies.

Numerical and laboratory models shed light on this variable dynamics at subinertial and lower frequencies (see Speich et al. 1996 or Gleizon et al. 1996, for instance) but there are important issues that have not been addressed yet. One of them is the coupling of the AJ and the WAG. The description of a swift AJ emerging from the Strait in the right direction to gently joint the WAG is not valid most of the time. The density-driven AJ usually impinges the basically geostrophic WAG under great angles for which a gentle coupling is not possible. In this case, the AJ must flow up the pressure gradient associated with the WAG. Simple arguments based on the Bernouilli equation indicate that an AJ flowing at the typical speed of 1 m s^{-1} could rise 5 cm up the sloping surface of the WAG before being stopped. Dynamic height differences at the sea surface between the center and the periphery in a developed WAG are typically 15–20 dyn cm (Lanoix 1974; Tintore et al. 1991; García Lafuente et al. 1998), which would stop the AJ before reaching the WAG center. The cyclonic bending shape of isolines of dynamic height of the WAG near the exit of the strait, shown in many maps of surface dynamic topography (Lanoix 1974; García Lafuente et

Corresponding author address: Jesús García Lafuente, Departamento de Física Aplicada II, E.T.S.I. Telecomunicación, Campus de Teatinos, s/n, 29071, Málaga, Spain.
E-mail: glafuente@ctima.uma.es

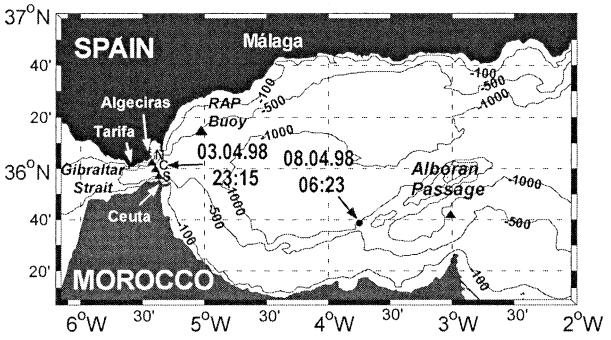

FIG. 1. Map of the Alboran Sea and Strait of Gibraltar showing the different monitoring sites (full triangles). Letters C, N, and S in the strait indicate the three mooring sites of the array deployed within CANIGO. RAP buoy and Alboran Passage positions, mentioned in the text, are also indicated. Dates in boldface are the start and end times of the experiment.

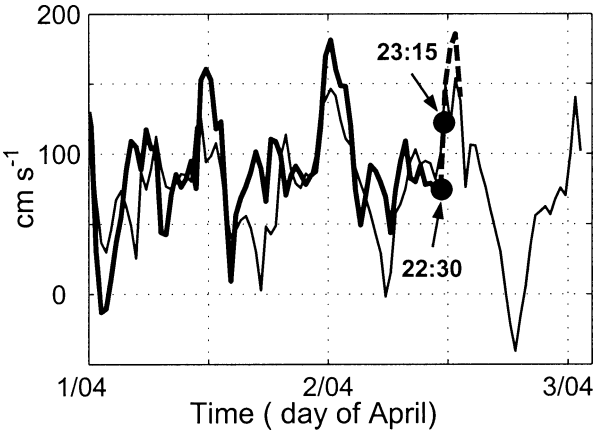

FIG. 2. Along-strait velocity recorded by the uppermost current-meter in sites C (thick line) and S (thin line). Thick dashed line is the velocity the first current-meter would have measured during the next 4 h after the accident, computed using tidal predictions and the good degree of correlation between observations in both sites. Solid dot at 2230 UTC is the last observation of the RCM, and the dot at 2315 UTC is an estimation of the along-strait velocity at the probable time of the accident.

al. 1998; Viúdez and Haney 1997; Viúdez et al. 2000), could be signatures of this rough assembly. With a developed WAG, a gentle assembly could be possible if the AJ leaves the strait under suitable angles of, say, 30° north of east (see last panel of Fig. 7 in this paper for a likely example). In either case, the final geostrophic adjustment of the AJ around the WAG has not been investigated yet.

Viúdez et al. (1998) analysed a set of hydrographic and acoustic Doppler current profiler (ADCP) observations that clearly depicted a nonsmooth coupling of the AJ and the WAG. They argued that the WAG would flow below 100 m in the area where it met the AJ, which would flow to the east above this depth crossing isolines of WAG dynamic height anomaly. They did not provide details of how the final adjustment would take place. That ageostrophic current would feed the gyre with recent Atlantic water (AW), compensating for mixing and losses through its bottom and probably making the WAG grow. Such a rough coupling could be associated with the time evolution (i.e., the growth) of the gyre. Obviously, the process would convert kinetic energy of the AJ into potential energy of the WAG and decelerate the AJ, facilitating its subsequent incorporation as a geostrophic current around the WAG. Other feasible process to remove kinetic energy from the AJ is the generation of submesoscale eddies in the area where both structures meet, which would be subsequently advected around the WAG and to the east. Although this kind of event has not been proven to take place yet, probably because the inherent difficulties to obtain reliable data in this complicated area, some of the dynamic topographies mentioned above could support their feasibility. On the other hand, the advection of submesoscale cyclonic eddies around the WAG have been reported from observations (La Violette 1984), from laboratory simulations (Gleizon et al. 1996) and from numerical models (Speich et al. 1996). In this paper we speculate about these ideas as the cause of the wavy path followed by a drifter released at the eastern exit of the Strait and recovered several days later at the eastern part of the WAG. First, we describe the observations (section 2) and the drifter trajectory (section 3). Section 4 investigates possible causes to explain this trajectory and put forward the formation and subsequent advection of a short-scale eddy as a possible mechanism for the observed path of the drifter.

2. Data

Most oceanographic data analyzed in this work were acquired as a result of an accident involving a mooring array of current meters monitoring flows at the eastern entrance of the Strait of Gibraltar (see Fig. 1 for details) on 3 April 1998. The mooring array was deployed within the European Union funded Project Canary Islands Azores Gibraltar observations (CANIGO). For unknown reasons, the center line (C in Fig. 1) broke a few meters below the uppermost Aanderaa-type current meter (RCM) placed at 40-m nominal depth. The last valid record was at 2300 UTC 3 April 1998. The next record at 2400 UTC gave a pressure corresponding to 1-m depth (surface) but the speed channel in the datalogger was not empty, implying that the accident did not happen at 2300 UTC but later. The speed of 38.6 cm s^{-1} registered at 2400 UTC is meaningless because the rotor disappeared in the accident (all records from 2400 UTC on 3 April onward had the threshold value for current speed) but it helps to estimate the time when it happened. The expected speed that the RCM had to have recorded at 2400 UTC should have been around 140 cm s^{-1} (see Fig. 2 and caption there). The registered speed was one-fourth of this value, which allows us to estimate 2315 UTC as the time of the accident.

After this time the subsurface buoy of 92.5-cm di-

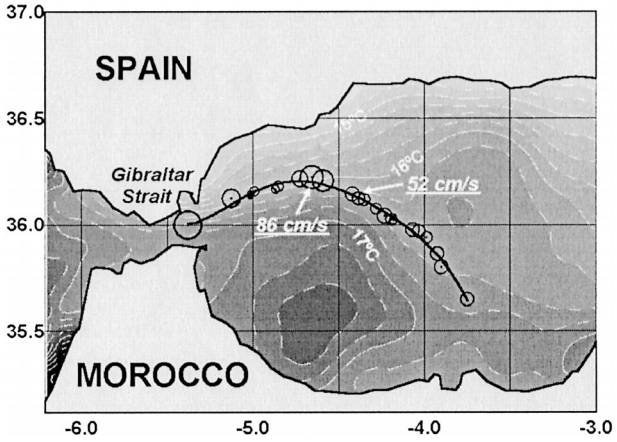

FIG. 3. Weekly composite SST image of the western Alboran Sea during the week. Thick line is the smoothed buoy path (SBP, see text) and circles indicate the computed velocity of the buoy from Eq. (1).

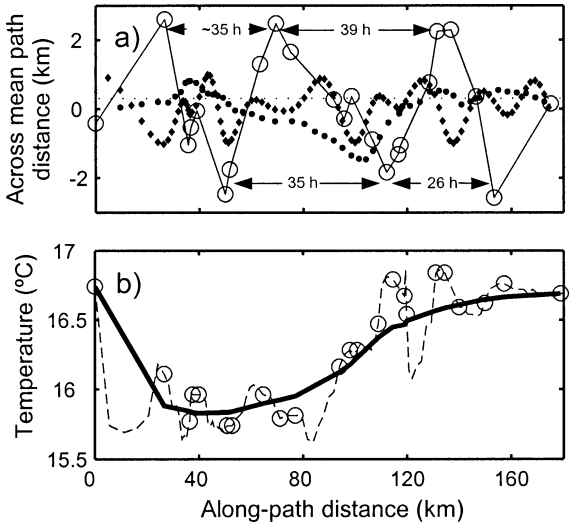

FIG. 4. (a) Departures of the buoy trajectory from the SBP. Elapsed times between consecutive extrema are shown. Circles correspond to tracked positions. Crosses indicate the predicted buoy departures produced by tidal currents in the Alboran Sea, and solid dots are the predicted buoy departures produced by wind drag acting on the emerged part of the buoy. (b) Hourly temperature data recorded by the RCM (dashed line) and temperature evaluated on the points belonging to the SBP (solid line). Circles correspond again to the tracked positions.

ameter and 320-kg buoyancy, with the RCM suspended 1 m below the buoy and the Argos transmitter attached to the buoy, became a drifter of opportunity whose consecutive positions were tracked by the Argos surveillance system. The temperature sensor of the RCM recorded near-surface water temperature (around 1-m depth). The experiment ended on 8 April 1998, when a rescue ship recovered the equipment that had traveled some 178 km embedded in the swift AJ (see Fig. 3).

Wind velocity over Alboran Sea and near-surface current speed during the time that the buoy was drifting were recorded by the Alboran Buoy of the Oceanographic Observational Network of Puertos del Estado, Spain [Red de Aguas Profundas (RAP)]. Current velocity data from the mooring array deployed at the eastern part of the Strait and in the Alboran Passage (see positions in Fig. 1) were also available as part of the mentioned monitoring program. Daily sea surface temperature (SST) infrared images during the period the buoy was drifting were downloaded from the German Remote Sensing Data Centre (DFD) Centre. Cloudy weather made the daily images during the experiment useless for comparison purposes, and a weekly composite of the week between 30 March and 5 April 1998 was used as reference.

3. Buoy trajectory

A total of 23 positions were tracked during the 103-h experiment, giving an average sampling of 4.5 h, although the actual sampling was irregular, ranging from 1.5 to 8 h. Instantaneous speed along the trajectory was computed from positions using the scheme

$$\frac{\partial s}{\partial t}(t_0) = \frac{1}{2}\left[\frac{s(t_0 + \Delta t_+) - s(t_0)}{\Delta t_+} + \frac{s(t_0) - s(t_0 - \Delta t_-)}{\Delta t_-}\right] + O(\Delta t_\pm), \quad (1)$$

where $s(t_0)$ is the position at t_0 and $s(t_0 \pm \Delta t_\pm)$ is the next/previous position. Speed at the first (last) position was computed as 2 times the first (second) term within brackets. They ranged from 29 to 84 cm s^{-1} and are shown in Fig. 3 as circles plotted around the positions of the buoy, radii being proportional to the computed velocity. Mean velocity was 48 cm s^{-1}, less than other reported values in the area (Lanoix 1974; García Lafuente et al. 1998; Viúdez et al. 2000).

A smoothed or ''mean'' trajectory of the buoy was obtained fitting the tracked positions to different order polynomials. A constraint was required that the trajectory at the starting point was due east to match the last observed velocity of the RCM before the accident ($u =$ 78 cm s^{-1}; $v = -2$ cm s^{-1}). Lowest-order polynomial verifying this condition satisfactorily was five. Figure 3 shows the smoothed buoy path (SBP) and illustrates the expected trajectory around the WAG.

Of particular interest is the wavy pattern around the SBP depicted by the consecutive positions of the buoy. Figure 4a shows the distance of each tracked position to the nearest point of the SBP (departures from the ''mean'' path), which makes the wavy pattern be much more apparent. The question then arises as to whether these departures are errors in the positioning of the buoy or, on the contrary, they have physical meaning. RCM temperature observations are useful to this aim. Figure 4b shows that they increased after the buoy drifted into the Alboran Sea, in good agreement with the background SST temperature map shown in Fig. 3. Should isotherms indicate geostrophic streamlines, the buoy

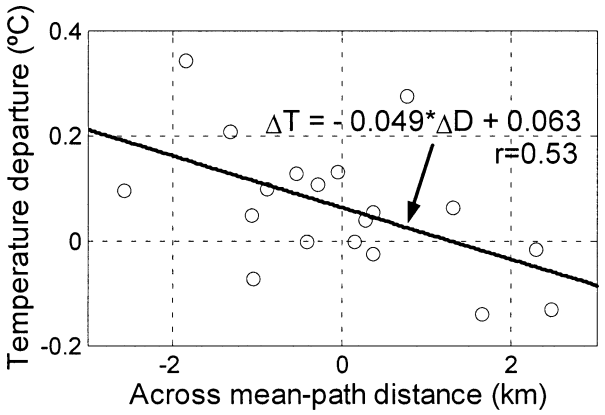

FIG. 5. Scatterplot of temperature departure against across-mean-path distance (SBP departures) and fitted straight line.

would have been ageostrophically displaced toward the centre of the WAG, a type of motion that has been already reported in this area (Viúdez et al. 1996, 1998).

Objective analysis was used to compute temperature on the SBP from RCM observations. SST image of Fig. 3 is not suitable to this aim because it is a weekly composite that introduces errors in determining instantaneous values. Temperature anomaly was computed by subtracting temperature at each tracked point from temperature at the nearest point on the SBP. Figure 5 shows the scatterplot of these anomalies versus across-SBP distance and the linear fit to the cluster of points. Although dispersion is high, points are clearly aligned in the expected direction. Even more, the coefficient of ΔD in the fitting indicates a cross-stream temperature gradient of -0.49°C km^{-1} in agreement with the gradient deduced from Fig. 3. The wavy trajectory is well supported by temperature observations and it is accepted as an actual feature of the surface circulation. Possible causes for it are discussed next.

4. Possible causes of the wavy path

a. Tides in the Alboran Sea

Tidal currents cause elliptic motions that will produce wavy Lagrangian trajectories when superposed onto a mean flow. Inside the Mediterranean Sea, the tide behaves like a standing wave slightly modified by rotation and, except for very specific places like straits, tidal motions are hardly ever important (Alberola et al. 1995). Tidal currents in the western Alboran Sea might be relevant due to the proximity of the Strait of Gibraltar. García Lafuente and Cano (1994) reported clockwise polarized M_2 tidal ellipses of around 7 and 1.5 cm s^{-1} for major and minor semiaxes, respectively, in the northwestern Alboran Sea near the Strait of Gibraltar. Another peculiarity of this area is the importance of diurnal species, which stems from the fact that the strait is nodal line for species 1 (García Lafuente et al. 1990), implying maximum amplitude of tidal currents. Consequently, tidal currents exhibit strong diurnal inequality, particularly during neap tides. Recent observations taken in RAP position (Fig. 1) give an M_2 tidal ellipse of 15.5 and -9.1 cm s^{-1} semiaxes oriented 36° from east with phase of 134° and a joint diurnal contribution of one-half of these amplitudes approximately (Alvarez Fanjul et al. 1999). Values are similar to those found in the surface layer at the eastern part of the Strait of Gibraltar (García Lafuente et al. 2000).

Harmonic constants from the Alboran–RAP site, which is close to the buoy trajectory, are used in the following discussion. Tidal ellipses of diurnal and semidiurnal constituents are roughly oriented along the AJ (Alvarez Fanjul et al. 1999). The magnitude of cross-AJ tidal current is then correctly represented by the minor semiaxis of the ellipses. Because of the standing-wave nature of the tide in the Mediterranean Sea, phase lag remains unchanged as the buoy moves downstream advected by the AJ. It implies northward (or southward) maximum departures from the mean trajectory approximately every 12.5 h, regardless of the position of the buoy. Crosses in Fig. 4a indicate the across-stream position of a water parcel jointly displaced by the predicted tidal and the reported main current. Even when it is only indicative (the reduction of tidal ellipses towards the east has not been considered, nor the curvature of the AJ), neither the size of across-SBP displacements nor their timing agree with the observed consecutive positions of the buoy. It could be that tides contribute to the small secondary peaks of cross-SBP displacements in Fig. 4a, but, overall, they must be discarded to explain the wavy trajectory.

b. Wind and wind stress

Wind is another candidate to explain the winding path. One possibility could be wind-induced inertial motions but the period of the wavelike path of Fig. 4a (around 35 h) is far from the inertial period at 36°N (20.4 h). Moreover, spectral analysis of velocity observations in RAP position and the Alboran Passage showed no signature of inertial motions. Similarly, transient states in the development of surface Ekman drift due to fluctuating wind intensity, which are related to inertial motions, should be discarded.

Another possibility is the direct drag that a fluctuating wind exerts on the exposed portion of the buoy. This force would be compensated by the friction drag exerted by water on the submerged part of the buoy, which moves at speed U_b relative to water under the action of wind. Hydrostatic equilibrium of the buoy–RCM ensemble is reached when 31% of the sphere volume is submerged (34% of the cross section of the sphere). Drag forces are assumed to be of the form $F_D = 0.5C_D A\rho U^2$ (Batchelor 1967), where ρ is the fluid density, A is the cross-section area exposed to the fluid, C_D is an appropriate drag coefficient, and U is the fluid velocity relative to the buoy. If wind drag is balanced

by water drag, the buoy speed relative to water is given by $U_b = [(C_{Da}/C_{Dw})(\rho_a/\rho_w)(A_a/A_w)]^{1/2}U_a$ (subscripts a and w refer to air and water, respectively). Using drag coefficients based on reasonable Reynolds number of the flows ($C_{Da} \approx 0.1$; $C_{Dw} \approx 0.6$: see Batchelor 1967, 340–342) and a cross-section area ratio of 1.94 (66% vs 34%), then $U_b \approx 0.02\ U_a$.

Wind observations in RAP station, which have been taken as representative of the area swept by the buoy, have been decomposed into along-SBP and across-SBP displacements at each point of the trajectory. The across-SBP wind, reduced by a factor of 2 to take into account the near surface speed reduction in the boundary layer, has been used to compute U_b and, hence, the across-SBP displacements that the wind drag could have explained (assumption has been made that the buoy followed wind changes instantaneously). They are plotted in Fig. 4a and show that predicted wind-induced departures do not match the observed ones either.

c. AJ–WAG interaction

The strong interaction between the density driven AJ and the WAG could be the origin of the observed wavy path. Some ideas supporting this hypothesis are presented now.

1) A SIMPLE DECOMPOSITION OF THE BUOY TRAJECTORY

The trajectory of the buoy could be separated into two simple motions: a circular-like motion within a short-scale eddy in which the buoy would have been trapped and the advection of the eddy downstream the WAG's periphery along the smoothed path indicated by the thick full line in Fig. 3. Advection velocity is estimated by means of Eq. (1) while the tangential velocity v_e of the circular-like motion is easily determined from Fig. 4a. The wavelike line implies a period of $T \approx 35$ h and a radius of $r \approx 2$ km for the circular motion, which gives $v_e = 2\pi r/T \approx 10$ cm s^{-1}, smaller than the advection speed around the WAG. It would be important to have an estimation of the relative vorticity inside the short-scale eddy. Under the simple hypothesis of an eddy with constant relative vorticity, ξ, the Stokes theorem applied to a closed circular streamline of radius r gives $\xi = 2v_e/r$ or $\xi \approx 10^{-4}$ s^{-1} for the values given above.

2) AJ RELATIVE VORTICITY

It is interesting to compare this value with Fig. 6a, which shows the spatially averaged relative vorticity of the AJ at the eastern part of the Strait of Gibraltar. Positive values are always found in the northern part of the jet with a mean close to $\xi \approx 10^{-4}$ s^{-1} and a clear tendency to increase with the along-strait velocity. In the southern half of the AJ, positive or negative values are equally probable with the opposite tendency to be negative for large values of the along-strait velocity. Figure 6b shows relative vorticity based on hourly observations, which include tidal variability and therefore are more interesting for the sake of the discussion of the event. Tides introduce some differences such as that relative vorticity in the northern half changes sign sporadically, but, overall, tendencies identified in Fig. 6a are maintained and linear coefficients for both sets of data are similar.

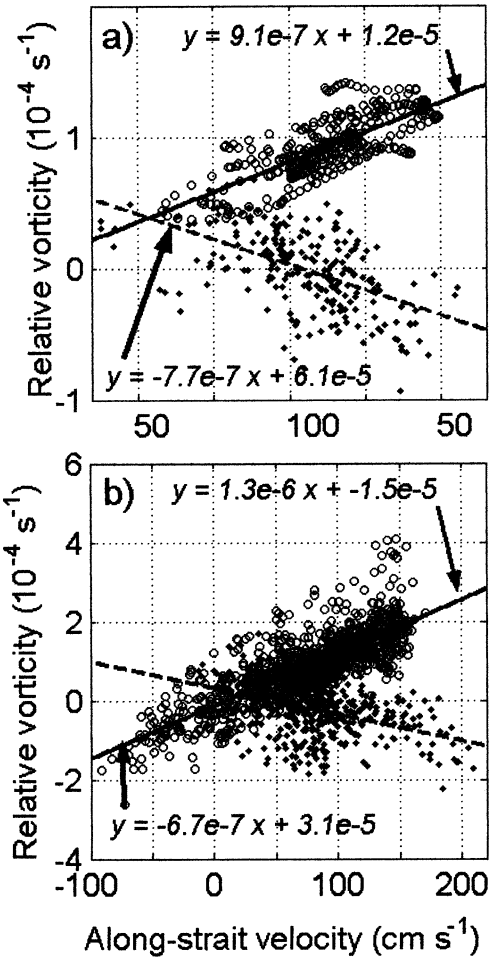

FIG. 6. (a) Low-passed (tidal free) relative vorticity computed from CANIGO observations as a function of the along-strait velocity observed at mooring C (see Fig. 1 for location). Open circles come from data of moorings N and C between Oct 1995 and May 1996, and diamonds are for data from moorings C and S from Aug 1997 to Apr 1998. (b) Hourly-based relative vorticity computations, which include tidal effect. Symbols have the same meaning as in (a).

For low along-strait velocity, the AJ tends to have homogeneous and low positive vorticity. For moderate to high speeds the tendency is for positive vorticity in the north and negative in the south, a distribution that favors the formation of dipole cyclonic/anticyclonic vortices at the exit of the strait. In either case, the strongly sheared flow of the northern part is a suitable source

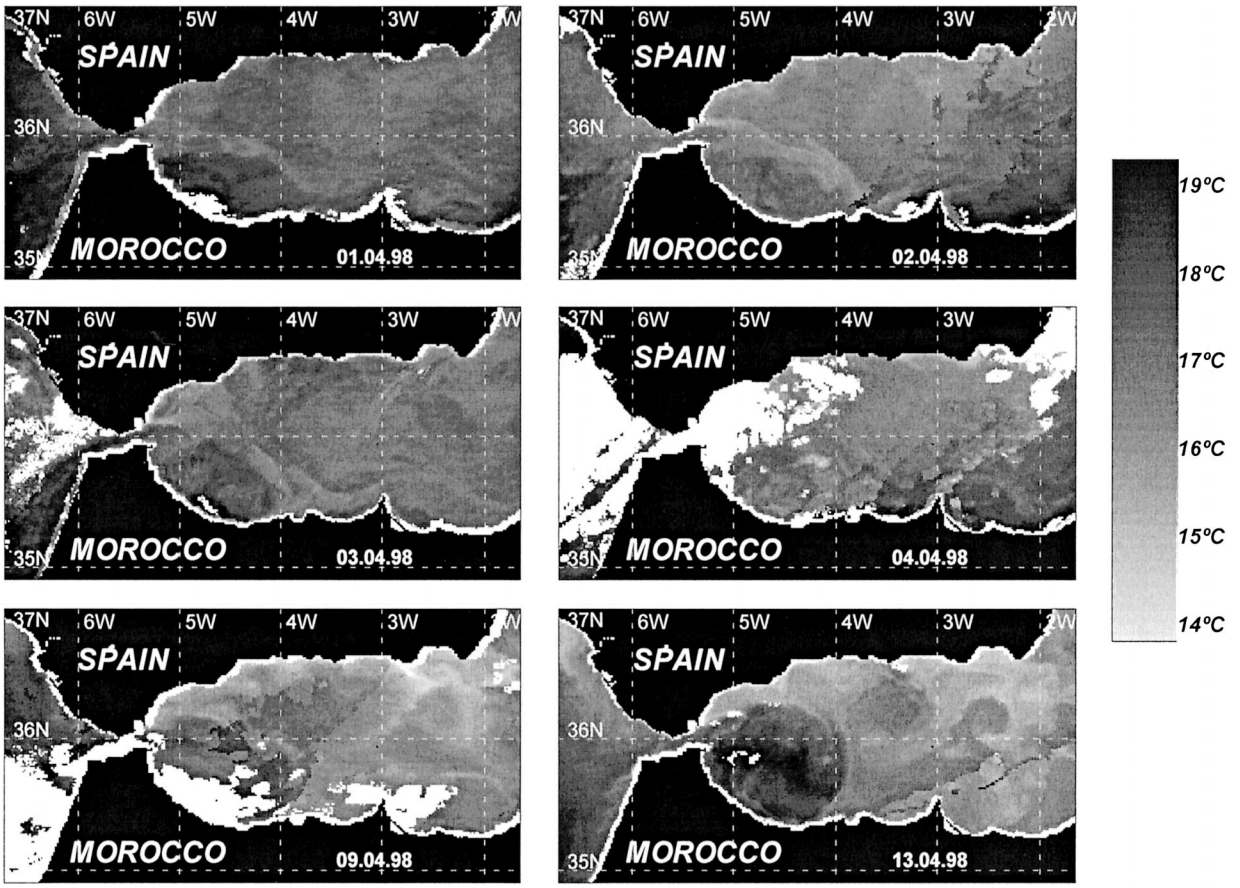

FIG. 7. SST images of the Alboran Sea during the days before (first four panels) and after (two last panels) the experiment. Dates are indicated in the lower part of each image. The size of the WAG largely increased during the days of the experiment.

of positive vorticity to generate a short-spatial-scale cyclonic eddy of the type mentioned above. The modulation that tides exerts on the AJ will change its vorticity distribution noticeably with tidal frequencies. Judging from the rapid variations of the along-strait velocity (Fig. 2), such changes may take place in very short time. It is particularly truth for the sharp increase of the AJ velocity during ebb tide, which would lead to the generation of pulses of dipolar relative vorticity.

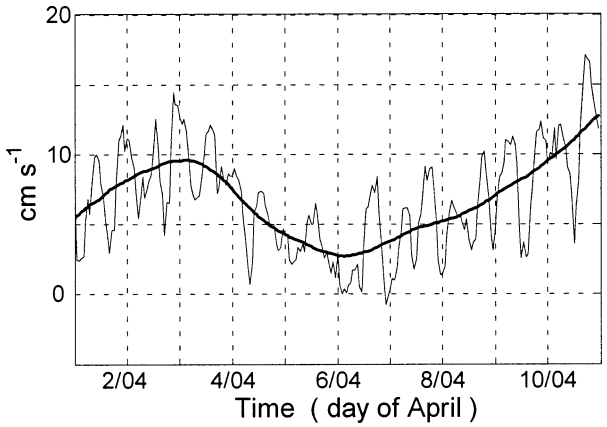

FIG. 8. Eastward velocity observed in Alboran Passage during the dates of the experiment. The thin line represents hourly velocities, and the thick line is the low-frequency (tidal free) contribution.

3) THE INCIDENCE ANGLE

It is argued now that the AJ and the WAG met under such an angle that a smooth coupling was not possible. This condition is fulfilled if (i) the WAG is developed enough to have near-northward flow along its western periphery at 36°N, 5°W in front of the eastern exit of the strait; and (ii) the AJ flows out of the strait almost due eastward.

SST images during the heavily clouded dates of the experiment were useless to depict the shape and size of the WAG. The sequence of SST images shown in Fig. 7 indicates, however, that it grew during the period that the buoy was drifting, increasing the amount of AW stored. Indirect evidence for that is also provided by the observations taken in Alboran Passage (Fig. 8), which shows a noticeable diminution of the eastward current starting on 3 April. Since this current is indicative of the AW transport to the eastern Mediterranean (Vargas

Yáñez et al. 2002), the conclusion would be that AW water had been feeding the WAG during that period.

The angle of the AJ as it flowed out of the strait slightly veered to the south, judging from the last velocity of $u = 78$ cm s^{-1}, $v = -2$ cm s^{-1} registered by the RCM (2300 UTC 3 April, which represents conditions at 2230 UTC because hourly sampling gives time-integrated speeds over the last hour). Only if the WAG was small and attached to the African coast south of 36°N a smooth AJ–WAG coupling would have been possible, a hypothesis not supported by the sequence of SST images of Fig. 7. On the other hand, the first tracked position of the buoy at 0612 UTC 4 April was 27.5 km at a bearing of 68° away from the released position, implying x and y displacements of 23.3 and 14.6 km, respectively. The x displacement during 7 h implies a mean velocity of 93 cm s^{-1}, not far from (but somewhat less than) that expected according to Fig. 2, but the y displacement implies a northward mean speed of 60 cm s^{-1} whose only explanation is the northward advection along the western part of the WAG. Obviously, the existence of a rather developed gyre is needed (or, at least and according to Figs. 7 and 8, a WAG in a growing phase), which would confirm that the AJ and the WAG met under a large angle that prevented a smooth coupling.

4) A LIKELY MECHANISM FOR EDDY GENERATION

As shown in Fig. 2, the accident took place when tidal currents were increasing. If the extrapolated along-strait velocity of $u \approx 120$ cm s^{-1} is valid, then Fig. 6b suggests dipolar relative vorticity in the AJ with strong positive values of 1.2×10^{-4} s^{-1} in the north and negative of -4×10^{-5} s^{-1} in the south. On the other hand, Viúdez and Haney (1997) showed that the outermost part of the WAG is a region of geostrophic positive relative vorticity ($2–3 \times 10^{-5}$ s^{-1}). When the AJ enters this region, the cyclonic vorticity of its northern part would be enhanced and the anticyclonic vorticity in the south reduced, favoring the formation of cyclonic vortices (whose length scale would be of the order of the width of the strait or 15 km) and inhibiting the formation of anticyclonic ones.

This conceptual model would suggest a frequent generation of cyclonic eddies, which does not seem plausible. Tidal pulses of dipolar vorticity mentioned above are put forward here as a potential mechanism to trigger the formation of those short-scale cyclonic vortices. The other important ingredient is the AJ–WAG angle. For great angles, the AJ has tendency to penetrate into the WAG, which slows down the jet and deflects it cyclonically, leaving clear signatures in some maps of surface dynamic topography [an interesting example of this cyclonic bending is shown in Fig. 2 of Viúdez and Haney (1997)]. Under these circumstances, the northern half of the jet would gain cyclonic curvature vorticity from its shear vorticity (see Viúdez and Haney 1997, for an extensive discussion on this mechanism), thereby facilitating the closure of streamlines, that is, the eddy formation. On the contrary, the southern half of the jet would diminish its negative vorticity, helping the direct ageostrophic feeding of the WAG with recent AW across WAG's isolines of dynamic height anomaly, in a manner that recalls the observations reported in Viúdez et al. (1998).

5. Summary and conclusions

The rather regular wavy path followed by the opportunity drifter around the WAG, described in section 2, could be explained by the formation of a cyclonic eddy at the location where AJ and WAG meet and by its subsequent advection along the WAG's periphery. Other invoked and, maybe, more intuitive mechanisms to explain the observations, like tidal currents in the Alboran Sea or wind forcing, are not able to provide a satisfactory explanation.

Two ingredients have been considered essentials for the eddy formation: (i) the fact that the AJ and the WAG meet under such a great angle that a smooth coupling of both structures is not possible, and (ii) the presence of large positive relative vorticity in the northern half of the AJ when it leaves the strait. The first ingredient requires the existence of a rather developed WAG, which implies a northward flow in the western WAG's periphery nearby the eastern exit of the Strait of Gibraltar, and also of the presence of a due east outflowing AJ at the Strait's exit. Both conditions were met at the time of the event discussed here. The presence of large positive relative vorticity is achieved by the strong tidal modulation the AJ undergoes within the strait. At the time of the accident, tidal currents sharply increased the AJ velocity (Fig. 2), leading to a large increase of the positive vorticity in the northern half of the AJ and the appearance of negative vorticity in the southern half.

The interaction of this AJ with the ambient positive vorticity of the WAG's periphery is a new source of positive vorticity that enhances (tends to cancel) the cyclonic circulation of the northern (southern) half of the AJ. Our final speculation is that the northern half of the AJ forms a short-scale cyclonic eddy at the zone where it meets the WAG while the southern half could flood the WAG ageostrophically, feeding it with recent AW as a result of this interaction. If as the AJ enters the Alboran Sea it veered to the north and facilitated a gentle assemble with the WAG, the final input of positive vorticity would not take place and the eddy would not be formed. On the other hand, with low along-strait velocities the vorticity in the southern half of the AJ is also positive and approaches the now reduced value in the northern half. Maybe that this almost constant and low ($+5 \times 10^{-5}$ s^{-1}) value throughout the width of the AJ and its diminished velocity favor the progressive northward bending of the AJ and its subsequent smooth

coupling with the WAG, even when it is well developed (see last panel of Fig. 7).

Acknowledgments. This work was partially supported by the European Commission through CANIGO Project (MAS3-PL95-0443) and by the Spanish National Program of Marine Science and Technology through Projects MAR95-1950-C02-01 and MAR99-0643-C03-01. Thanks are given to the captain and crew of SALVAMAR rescue ship from Málaga port that helped us to recover the released instrumentation.

REFERENCES

Albérola, C., and Coauthors, 1995: Tidal currents in the Western Mediterranean Sea. *Oceanol. Acta,* **18,** 273–284.

Alvarez Fanjul, E., M. Alfonso, O. Serrano, and M. I. Ruiz, 1999: Proyecto RAYO. Informe de datos de la boya de Alborán (1998). Clima Marítimo Tech. Rep. (in Spanish), Puertos del Estado, Madrid, 68 pp.

Batchelor, J. K., 1967: *An Introduction to Fluid Dynamics.* Cambridge University Press, 615 pp.

Candela, J., C. D. Winant, and H. L. Bryden, 1989: Meteorologically forced subinertial flows through the Strait of Gibraltar. *J. Geophys. Res.,* **94,** 12 667–12 679.

García Lafuente, J., and N. Cano, 1994: Tidal dynamics and associated features of the northwestern shelf of the Alboran Sea. *Cont. Shelf Res.,* **14,** 1–21.

——, J. L. Almazán, F. Castillejo, A. Khribeche, and A. Hakimi, 1990: Sea level in the Strait of Gibraltar: Tides. *Int. Hydrogr. Rev.,* **47,** 111–130.

——, N. Cano, M. Vargas, J. P. Rubín, and A. Hernández Guerra, 1998: Evolution of the Alboran Sea hydrographic structures during July 1993. *Deep-Sea Res.,* **45A,** 39–65.

——, J. M. Vargas, F. Plaza, T. Sarhan, J. Candela, and B. Baschek, 2000: Tide at the eastern section of the Strait of Gibraltar. *J. Geophys. Res.,* **105,** 14 197–14 213.

——, E. Alvarez Fanjul, J. M. Vargas, and A. W. Ratsimandresy, 2002: Subinertial variability in the flow through the Strait of Gibraltar. *J. Geophys. Res.,* **107**, 3168, doi:10.1029/2001JC0011004.

Gleizon, P., G. Chabert-d'Hières, and D. Renouard, 1996: Experimental study of the Alboran Sea gyres. *Oceanol. Acta,* **19,** 499–511.

Heburn, G. W., and P. E. La Violette, 1990: Variations in the structure of the anticyclonic gyres found in the Alboran Sea. *J. Geophys. Res.,* **95,** 1599–1613.

Lanoix, F., 1974: Project Alboran. Etude hydrologique et dynamique de la Mer d'Alboran. NATO Tech. Rep. 66, Brussels, 39 pp. plus 32 figs.

La Violette, P. E., 1984: The advection of mesoscale thermal features in the Alboran Sea gyre. *J. Phys. Oceanogr.,* **14,** 550–565.

Parrilla, G., and T. H. Kinder, 1987: Oceanografía Física del Mar de Alborán. *Bol. Inst. Esp. Oceanogr.,* **4,** 133–165.

Sarhan, T., J. García Lafuente, M. Vargas, J. M. Vargas, and F. Plaza, 2000: Upwelling mechanisms in the northwestern Alboran Sea. *J. Mar. Syst.,* **23,** 317–331.

Speich, S., G. Madec, and M. Crepon, 1996: A strait outflow circulation process study: The case of the Alboran Sea. *J. Phys. Oceanogr.,* **26,** 320–340.

Tintoré, J., D. Gomis, S. Alonso, and G. Parrilla, 1991: Mesoscale dynamics and vertical motions in the Alboran Sea. *J. Phys. Oceanogr.,* **21,** 811–823.

Vargas Yáñez, M., F. Plaza, J. García Lafuente, T. Sarhan, J. M. Vargas, and P. Vélez Belchi, 2002: About the seasonal variability of the Alboran Sea circulation. *J. Mar. Syst.,* **35,** 229–248.

Viudez, A., and R. L. Haney, 1997: On the relative vorticity of the Atlantic jet in the Alboran Sea. *J. Phys. Oceanogr.,* **27,** 175–185.

——, J. Tintoré, and R. L. Haney, 1996: Circulation in the Alboran Sea as determined by quasy-synoptic hydrographic observations. Part I: Three-dimensional structures of the two anticyclonic gyres. *J. Phys. Oceanogr.,* **26,** 684–705.

——, J. M. Pinot, and R. L. Haney, 1998: On the upper layer circulation of the Alboran Sea. *J. Geophys. Res.,* **103,** 21 653–21 666.

——, R. L. Haney, and J. T. Allen, 2000: A study of the balance of horizontal momentum in a vertical shearing current. *J. Phys. Oceanogr.,* **30,** 572–589.